Vertical energy filtering of ultra-cold neutrons by a bounded gravitational potential

C.D. Raskin and R.B. Doak*

Department of Physics and Astronomy, Arizona State University, Tempe, AZ 85287-1504

(Received 13 March 2002; published)

The gravitational trapping of ultra-cold neutrons above a flat mirror surface is analyzed from the perspective of simple quantum mechanics. An existing model is refined to fully account for restriction of motion in the vertical plane by a scatterer/absorber plate situated above and parallel to the mirror. This yields subtle but real differences in transmission threshholds for neutron flux through the mirror-absorber gap. The device functions as a discrete mode, low-pass energy filter for motion in the vertical plane.

PACS Codes: 03.65.-w, 28.20.-v, 03.75.-b

Simple models can be essential aids to conceptual understanding, providing a framework upon which to build more complete theoretical analysis. A simple model should incorporate the relevant and vital science while identifying and disregarding peripheral details. Separating the wheat from the chaff is often not a simple matter. Ultimately this balance is assessed by the predicative power of the model and by the clarity and correctness of insight it delivers. The model must correctly explain fundamental observations, for example the positions of features in experimental spectra, but need not necessarily deliver more complex information, such as peak shapes and intensities. In this paper we refine the simple model proposed by Nesvizhevzky et al. [1] to elucidate their beautiful measurements of ultra-cold neutrons (UCN) "bouncing" along a flat horizontal surface, confined vertically by gravity. Those authors invoke spatial filtering of the neutron wave function to explain their data, using for that purpose the wave functions of a linear gravitational potential bounded below by an infinite hard wall. More tenable from the perspective of fundamental quantum mechanics is a gravitational potential bounded above as well as below. We explore this double hard wall gravitational potential and develop a simple scheme to more fully understand the experimental measurements.

The experimental arrangement is depicted schematically in Fig. 1. Ultra-cold neutrons are directed into a vertical gap between a flat, ultra-smooth glass surface below and a flat, micro-roughened glass surface above. A detector at the far end of the gap monitors neutron throughput as the gap height a is varied. Within a classical description, the ultra-cold neutrons "bounce" along the upper surface of the lower plate (the "mirror"), subject to incoherent scattering and absorption at the lower surface of the upper plate (the "absorber"). The experimental measurements show a deficit of throughput at small gap heights and indeed no transmission at all for gaps of less than ~15 μm. The throughput increases in a stepwise fashion as the gap is widened, eventually merging with the classically predicted flux for gaps larger than ~50 μm. These data are interpreted as a manifestation of the quantum mechanical nature of the neutron, specifically that no transmission is expected if the gap "is smaller than the spatial width of the lowest quantum state" [1]. A stepwise increase in transmission is predicted when the gap is "equal to the spatial width of the lowest quantum

* Email: bdoak@asu.edu

state," followed by constant throughput until the gap reaches "the spatial width of the second quantum state," yielding a second stepwise rise, and so forth. This simple picture does indeed predict discrete, stepwise increases in the neutron throughput. However, the model invokes neutron wave functions of the pure gravitational potential [1, 2] and thereby disregards changes in the potential well introduced by the absorber. A more detailed quantum treatment by the ILL group reproduces the stepwise increases in throughput [1]. Nonetheless, an obvious question arises: Can a simple yet more correct and robust model be found? We suggest that the necessary modifications are easily made. Only two are needed: The first is to emphasize the role of the absorber as an energy filter rather than a spatial filter. The second is to identify the correct set of eigenstates and to recognize that these shift in shape and energy with gap size.

Adopting the x and z axes of Fig. 1 and assuming independence of horizontal and vertical motions, the time-independent wave function of a neutron in the device separates to yield

$$y(x, y, z) = y_{vert}(z)\, y_{horiz}(x, y) \quad . \tag{1}$$

In the horizontal direction, the Schrödinger equation is that of a simple traveling plane wave. In the vertical direction, with no absorber plate present and assuming no penetration of the neutron into the glass plate, the situation can be modeled as an infinite hard wall at $z = 0$ plus a linear gravitational potential $V(z) = m\, g\, z$ above the hard wall. The time-independent Schrödinger equation in the vertical direction is then

$$-\frac{\hbar^2}{2m}\frac{d^2 y_{vert}(z)}{dz^2} + m g z\, y_{vert}(z) = E_z\, y_{vert}(z) \quad . \tag{2}$$

This is a standard eigenvalue problem of elementary quantum mechanics [3]. Redefinition of z yields the Airy equation, with solutions given by the Airy function, $Ai(x)$. Denoting the properly normalized eigenfunctions as $f_z^n(z)$ and the associated energy eigenvalues as E_z^n, it follows that the vertical wave function is equal to one of the $f_z^n(z)$

$$y_{vert}(z) \in f_z^n(z) = A_n\, Ai\left[\left(\frac{2}{mg^2\hbar^2}\right)^{2/3}\left(m g z - E_z^n\right)\right] \quad , \tag{3}$$

or to some linear combination thereof. A_n is a normalization constant. The E_z^n are determined by the hard wall boundary condition $y_{vert}(0) = 0$. Being eigenfunctions of a Hermitian operator, the $f_z^n(z)$ constitute a complete, orthogonal basis set. The discrete energy spectrum implies discrete classical velocity components v_z in the vertical direction,

$$v_z \in \sqrt{\frac{2E_z^n}{m}} \quad . \tag{4}$$

The lowest five energy eigenvalues for a neutron (mass m =1.0087 AMU) are E_z^n = 1.406, 2.459, 3.320, 4.081, and 4.777 peV. The wave functions and energies of Eqn. (3) pertain only to the vertical component of motion and only to the case of a pure gravitational well bounded below by an infinite hard wall. In particular these results do not apply with the absorber in place, since the potential no longer has the simple gravitational form $V(z) = m\,g\,z$ in the region z ³ a .

Energy selective attenuation by the absorber is most easily broached in a classical picture, treating the neutrons as if they were point particles following simple parabolic trajectories as they bounce elastically along the mirror surface. Consider a neutron rebounding from the mirror with an initial vertical velocity component v_z . Below a critical value v_z*, the neutron cannot reach the absorber, situated a height a above the mirror. The associated critical energy in the z-direction is simply

$$E_z * = \frac{1}{2} m \left(v_z *\right)^2 \; = \; m\,g\,a \quad . \tag{5}$$

Neutrons leaving the mirror with $E_z < E_z$* "bounce" unhindered through the gap. Those with E_z ³ E_z* reach the absorber where they undergo incoherent scattering at the micro-roughened surface. This re-directs their velocity and causes them to be absorbed. The process effectively eliminates all neutrons that reach the absorber surface, as verified by the fact that the measured transmission is essentially zero for sufficiently small gap heights. Upon moving from this classical picture to a correct quantum mechanical description, it is clear that E_z* will remain a relevant physical quantity. It no longer defines an absolute cut-off energy, however, but rather a pass energy above which the transmitted intensity dies off in an exponential manner. Thus the device functions as a low-pass filter for $E_z < E_z$* . Moreover it is tunable by selecting E_z* through variation of the gap height a. Coupled with the discrete spectrum of energy eigenvalues of a neutron within the gap, this explains both the deficit in transmission of the device at small gap height and the stepwise increase in transmission as the gap is increased: A step in transmittivity must occur when the critical energy E_z*(a) reaches and exceeds one of the allowed energy levels E_z^n. To complete the analysis, it remains only to identify the relevant energy eigenvalues.

Any arbitrary wave function $y_{vert}(z)$ can be expanded in an appropriate basis, such as the Airy functions $f_z^n(z)$ of the semi-infinite gravitational potential,

$$y_{vert}(z;x) = \sum_n c_z^n(x) f_z^n(z) \quad . \tag{6}$$

With the absorber in place, the potential for z ³ a is not the simple linear potential. The relevant eigenfunctions are therefore not the Airy functions, although the correct eigenfunctions could always be expressed as linear combinations of those. Mathematically, the presence of the absorber can be modeled by introducing a complex potential in the absorber region, the imaginary portion of which gives rise to a negative imaginary component of wave vector and hence to an exponential decay in wave function amplitude in that region. However, this clearly moves into the realm of more advanced modeling. Is there not a simpler way of viewing this problem? The answer is yes, recognizing that the absorber reduces to zero, in the course of a neutron's transit through the device, the probability of finding the neutron in the absorber region, z ³ a . This requires, as illustrated schematically in Fig. 2, that $y_{vert}(z)$ in the absorber region decrease with x , to eventually vanish entirely for z ³ a before reaching the end of the device at $x = L$. (In addition, the wave function changes in shape as it passes along the gap, losing features of high curvature as will become clear.) Accordingly, the coefficients in Eqn. (6) depend on x, as indicated. If only the output characteristics of the device are sought, then only the output form $y_{vert}(z; L,a)$ is needed. Note that the vertical wave function takes on this special form only at large x and that this form depends on the gap separation a. Hence L and a have been explicitly included as parameters of this final wave function form.

The end wave function $y_{vert}(z; L,a)$ could be expanded in the Airy eigenstates $f_z^n(z)$ but this is not the most useful basis. To yield a zero in $y_{vert}(z; L,a)$ at both $z = 0$ and $z = a$ an admixture of at least two $f_z^n(z)$ is needed, even for the lowest energy state. The lowest energy expectation value is an average of these two eigenvalues, of probabilities $|c_z^n(x)|^2$, and must lie above the lowest Airy eigenvalue E_z^1. The state energy will increase with decreasing gap a due to the need for higher order $f_z^n(z)$ components to move the upper zero to lower z. An alternative basis set allows a more direct analysis. That basis is easily identified by the usual quantum mechanics homology: Since $y_{vert}(z; L,a)$ is identically zero in the region z ³ a, the form of the potential in there is not only irrelevant to that function but can be replaced by an infinite potential. The characteristics of $y_{vert}(z; L,a)$ are therefore determined by the gravitational well, $V(z) = m\,g\,z$, bounded both below and above by infinite hard walls at $z = 0$ and $z = a$, respectively. The eigenfunctions of this double hard wall gravitational potential, which we denote $c_z^n(z; a)$, provide the desired basis set. They form a complete orthogonal basis for any wave function that is identically zero outside of the domain $0 < z < a$. Consequently, any arbitrary $y_{vert}(z; L,a)$ can be expanded in the $c_z^n(z; a)$. The associated energy eigenvalues, denoted $e_z^n(a)$, comprise the set of energy expectation values relevant to a measurement of $y_{vert}(z; L,a)$. The lowest energy state is the ground state $c_z^1(z; a)$, admixed with no other $c_z^n(z; a)$.

The eigenfunctions $c_z^n(z; a)$ and the associated energy eigenvalues $e_z^n(a)$ are easily obtained by numerical integration [4]. Calculated values for the lowest five eigenvalues are plotted in Fig. 3 as a function of the mirror-absorber separation a. At sufficiently large a the curves level off at the eigenvalues of the semi-infinite gravitational potential, as must be the case. The curves rise as the gap is decreased. This is also expected, since greater curvature (and hence via the Schrödinger equation larger $|e_z^n(a) - m\,g\,z|$) is needed to bring the wave function to zero at both ends of a decreased spatial extent. At very small z the doubly-bounded gravitational potential approximates a simple infinite square well and the energy eigenvalues must rise with the a^{-2} dependence of that limiting case. If the upper surface of the gap were totally reflecting rather than totally absorbing, viable solutions would exist even at very small z, albeit only with high energy. The presence of the absorber turns these real wave functions into evanescent functions for sufficiently large $e_z^n(a)$.

The overall picture to explain the steps in transmittivity of the ILL device is constructed by superimposing on Fig. 3 the lowpass energy $E_z{}^*(a) = m\,g\,a$ and recognizing that the absorber removes eigenstates of energy greater than $E_z{}^*(a)$. At sufficiently small z this precludes all states and the device is fully opaque. The intersection of the $e_z^1(a)$ curve with the $E_z{}^*(a)$ line at a = 15.8 μm marks the critical gap size to allow transmission of the ground state eigenfunction. A step from zero to finite transmission is expected at this gap size. Likewise, a second step should occur at the intersection $e_z^2(a) = E_z^*(a)$, namely at $a = 25.9$ μm, and similarly in sequential order for each successive intersection of the $e_z^n(a)$ curves with the $E_z^*(a)$ line. The predicted critical gap heights are superimposed on the experimental data in Fig. 4. The agreement with the measured rises in signal is seen to be quite good. Recall that these critical energies are quantum mechanically "corner" values rather than absolute thresholds and should yield exponential rises rather than abrupt steps. Note also that the elimination of high energy eigenstates will alter the wave function as it passes through the device, eliminating high curvature features of the vertical wave function as suggested in Fig. 2.

What do we learn from this exercise? The simplicity of the model, the clarity of the predictions, and the agreement with the experimental data would indicate that the model has struck the right balance between "wheat" and "chaff." The stepwise rise of the measured neutron throughput can confidently be assigned to the action of the absorber as a low pass filter for neutron energies $E_z < m g a$ and to the resulting modification of the output eigenstate spectrum. The stepwise rises in throughput require both selection and filtering. Replacement of the absorber with a second mirror would not yield a throughput deficit at small gap heights. This understanding bears on analogous experiments with other particles, for example helium atom transmission through narrow slits. Highly directional and extraordinarily intense superfluid helium beams are now available at 15 m/s from a superleak nozzle [5]. That velocity could easily be further reduced by gravitational deceleration. Superfluid-surface scattering from solid surfaces is completely uncharted experimental territory, but coherent specular scattering is expected at sufficiently low perpendicular velocity. Atoms are non-penetrating so that an atomically rough surface would be employed to attenuate by incoherently scattering, exactly as in the ILL device. Trapping into not just the gravitational bound states but also into bound states of the gas-surface potential well would considerably enrich the bound state wave functions.

The double hard wall model predicts that both the neutron measurement and analogous experiments with other particles should be relatively insensitive to the angular and energy distributions of the incident beam. High E_z resolution of the incident beam is not needed to produce a throughput deficit at small gap height. Thus the incident energy distribution is constrained only by the need for full reflection from the mirror surface and for complete elimination of all neutrons that strike the absorber surface. To a beam having high resolution in its E_z distribution, the device would be a variable band pass filter (if not diffraction-limited by the gap size). By adding to Fig. 3 a horizontal line (or band) at the value (or spread) of the E_z distribution in the incident beam, that case is easily analyzed. The E_z output spectrum of the device is controllable and predictable in any case. Experimental measurement of the spectrum of the device would offer an independent means of confirming and extending the modeling.

Note that the $e_z^n(a)$ curves of Fig. 3 become, in the absence of an upper boundary condition, simple straight-line energy-independent extensions of their large a asymptotes. The intersections of that family of lines with $E_z^*(a) = mga$ delivers the critical gap sizes predicted by the semi-infinite gravitational potential of Nesvizhevzky et al. [2], namely 13.7, 24.0, 32.4, 39.8, and 46.6 μm for the lowest five values. Experimentally, the doubly-bounded well predicts 15.8, 25.9, 34.3, 41.8, and 48.6 μm as listed on Fig. 3. The corrections are small but real and possibly accessible to more precise experimental measurement. More significant is the energy dependence of the $e_z^n(a)$ curves of Fig. 3, emphasizing that energy filtering plays a critical role in determining the transmission characteristics of the device. Neglect of the upper boundary condition removes this energy dependence entirely.

More refined theoretical treatment should clearly involve a 2D numerical calculation based on a complex potential appropriate to the absorber. There is an obvious mapping onto the physics of an "atom optics" waveguide: A refractive index for neutrons (or any other particle) can be defined on the basis of the potential $V(z)$ and the total energy E,

$$n(z) = \sqrt{1 - \frac{V(z)}{E}} \quad . \tag{7}$$

The ILL device corresponds to a planar waveguide having a graded index of refraction in its core and an absorbing wall. By varying the position of the absorber the impedance characteristics of the waveguide are altered, changing its bandpass spectrum.

Acknowledgements

We are grateful to J.C.H. Spence for bringing the ILL work to our attention and to K.E. Schmidt for valuable discussions and a careful reading of the manuscript. This analysis was initiated as an extracurricular undergraduate class project by one of the authors (C.D.R) in conjunction with course PHY-315, Quantum Physics II, at Arizona State University.

Figure Captions

Fig. 1. Schematic drawing of the ILL ultra-cold neutron (UCN) device [1]. The force of gravity acts in the negative z-direction. Two flat parallel plates, a neutron lower mirror and an upper neutron scatterer/absorber, are separated vertically by a gap of height a . Ultra-cold neutrons (UCN) are incident from the left with a finite spread of velocities in the vertical direction. A detector to the right measures the flux of neutrons though the gap.

Fig. 2. Schematic depiction of the changing shape of the vertical portion of a neutron wave function, $y_{vert}(z)$, as it travels from the entrance ($x = 0$), to an intermediate position, and on to the exit ($x = L$) in the presence of an absorbing material in the region z ³ a . Surface scattering/absorption in the ILL device forces $|y_{vert}(z;x)|^2$ to zero in the absorber region, but bulk absorbtion (dashed line) could yield the same overall outcome.

Fig. 3. Energy eigenvalues $e_z^n(a)$ of a gravitational potential well bounded by an infinite hardwall both below ($z = 0$) and above ($z = a$), plotted as a function of the gap height a . The index $n = 1$ labels the ground state. Superimposed upon this family of curves is the lowpass energy, $E_z{*} = m\ g\ a$ of the ILL device. Classically, neutrons having an energy in the vertical plane of less than $E_z{*}$ at position $z = 0$ pass unhindered through the device. The intersection of each eigenvalue curve with this line therefore marks a critical gap height, listed on the figure.

Fig. 4. Measured neutron throughput of the ILL device [1]. The solid line curve gives the classically expected throughput. Vertical bars mark critical gap heights at which stepwise jumps in transmissivity are predicted by the curve intersections of Fig. 3. The measured data do indeed exhibit distinct steps at the bars and recognizable plateaus between the bars.

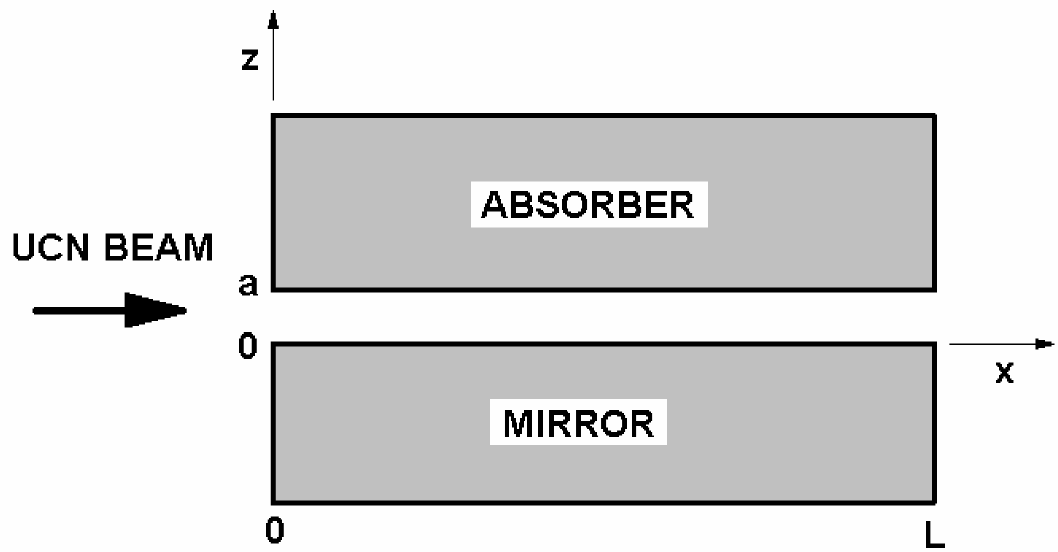

Raskin and Doak, Fig. 1.

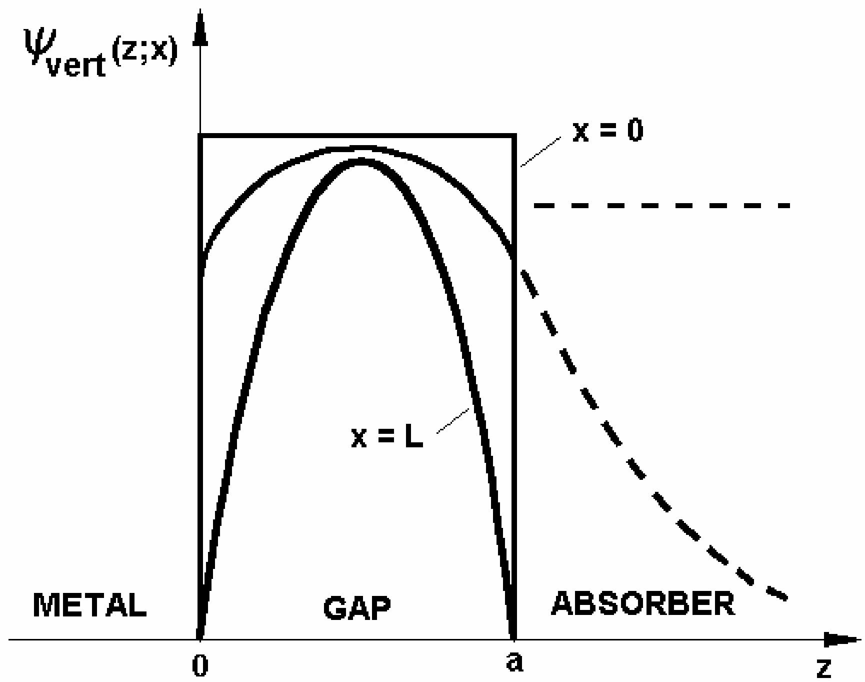

Raskin and Doak, Fig. 2.

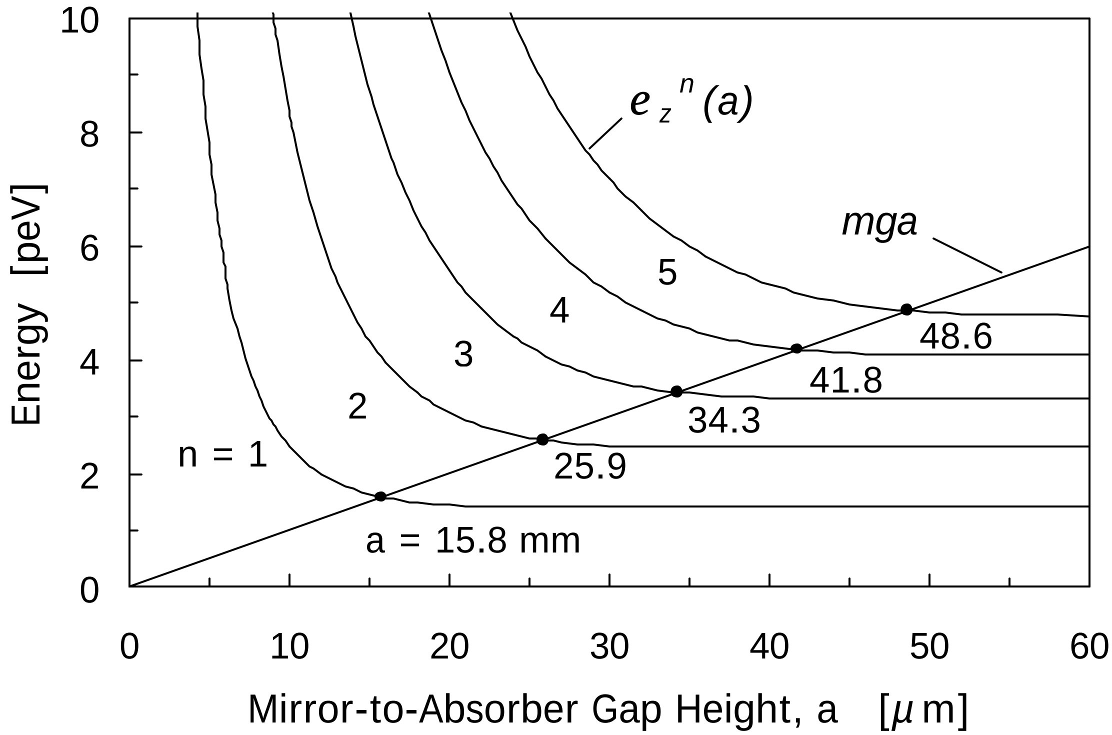

Raskin and Doak, Fig. 3

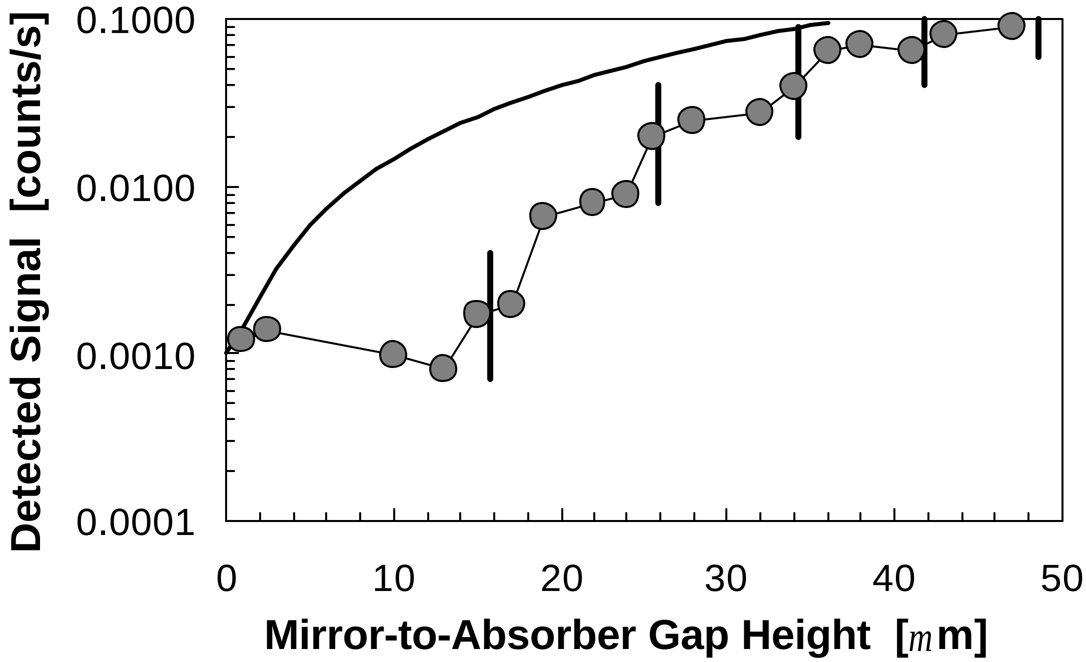

Raskin and Doak, Fig. 4

References

[1] V.V. Nesvizhevsky, H.G. Börner, A.K. Petukhov, H. Abele, S. Baeßler, F.J. Reuß, T. Stöferle, A. Westphal and A.M. Gagarski, G.A. Petrov, and A.V. Strelkov, Nature **415**, p. 297 (2002).

[2] V.V. Nesvizhevsky, H. Börner, A.M. Gagarski, G.A. Petrov, A.K. Petukhov, H. Abele, S. Bäßler, T. Stöferle, and S.M. Soloviev, Nuc. Instrm. Meth. **A 440**, p. 754 (2000).

[3] N.Zettili, *Quantum Mechanics* (Wiley, Chichester, 2001), p. 261.

[4] Particularly transparent is a spreadsheet calculation based on the "shooting method" and employing the simplest second order difference equation corresponding to Eqn. (2). See \\PHYASTWEB\HOMEPAGES\rbdoak\SPREADSHEETS. Recognizing that the outer hard wall may lie in a classically forbidden region, the integration must start at $z = a$ and step into the classically allowed region at small *x*. The starting amplitude at $z = a$ is set to zero as demanded by the upper hard wall boundary condition. "Shots" are then taken and the energy varied until the energy is found that yields a wave function amplitude of zero at $z = 0$. A built-in spreadsheet "Solver" macro automates this iteration.

[5] R.E. Grisenti and J.P Toennies, *Int. Symp. on Quantum Solids and Fluids, QFS_2001*, July 22-27, 2001, (unpublished).